Optical anisotropy of (001)-GaAs surface quantum wells

L. F. Lastras-Martínez,[1,2,*] D. Rönnow,[1] P. V. Santos,[1,3] M. Cardona,[1] K. Eberl[1]
[1]*Max-Planck-Institut für Festkörperforschung, Heisenbergstr. 1, D-70569 Stuttgart, Germany*
[2]*Instituto de Investigación en Comunicación Optica, Universidad Autonóma de San Luis Potosí, Alvaro Obregón 64, San Luis Potosí, Mexico*
[3]*Paul-Drude-Institut für Festkörperelektronik, Hausvogteiplatz 5-7, D-10117 Berlin, Germany*
(Received 26 May 2001; published 28 November 2001)

We report a reflectance difference spectroscopy (RDS) study of the optical anisotropy of GaAs:(001) surface quantum wells consisting of a thin GaAs layer (3–30 nm thick) embedded between an arsenic reconstructed surface and an AlAs barrier. The RDS spectra display anisotropic contributions from the free surface and from the GaAs/AlAs interface. By comparing RDS spectra for the $c(4\times4)$ and (2×4) surface reconstructions, we separate these two contributions, and demonstrate that the anisotropy around the E_1 and $E_1+\Delta_1$ transitions comprises a component originating from modifications of bulk states near the surface. The latter is attributed to anisotropic strains induced by the surface reconstruction. The experimental data are well described by a model for the RDS response of the multilayer structures, which also takes into account the blue energy shifts and the changes in oscillator strength of the E_1 and $E_1+\Delta_1$ transitions induced by quantum-well confinement.

DOI: 10.1103/PhysRevB.64.245303 PACS number(s): 78.20.−e, 78.66.−w, 78.90.+t

I. INTRODUCTION

Reflectance difference/anisotropy spectroscopy[1] (RDS/RAS), a technique that measures differences in the reflection coefficient for polarization along two orthogonal surface directions, was successfully used as an optical probe for the study of surfaces and interfaces in cubic semiconductors. RDS spectra have been reported to include components due to local-field effects,[2,3] surface reconstruction,[4–7] molecule adsorption,[8] spatial dispersion,[9] electro-optic effects,[10,11] and surface dislocations.[12] RDS studies of GaAs quantum wells (QW's) embedded between asymmetric barriers were also reported.[13,14] A number of applications were mentioned in the literature, among them *in situ* characterizations of epitaxial growth processes, both by molecular-beam epitaxy (MBE) (Ref. 15) and metal-organic chemical vapor deposition,[16] which exploit the sensitivity of RDS spectra to surface reconstructions. RDS was also used for the measurement of doping levels during the epitaxial growth of GaAs and $Ga_{1-x}Al_xAs$ by detecting the breakdown of the cubic symmetry in the presence of a surface electric field.[17]

Despite intensive investigations, there is a controversy about the physical origin (bulk or surface) of the different components of the RDS signal. The reconstruction of semiconductor surfaces leads to the formation of bonds not present in the bulk. Typical examples are the As or Ga dimers found on the different reconstruction of the (001) GaAs surface. Electronic states associated with the dimers are expected to be strongly localized near the surface.[18] Since the dimers have a preferential orientation, electronic transitions involving these states are expected to be highly anisotropic. In addition, reconstruction induces slight changes in atomic positions in the atomic layers close to the surface, thus producing a strain field. The latter, together with the dimers, modify bulk electronic states near the surface, leading to the formation of surface resonances. Contrary to previous conjectures,[4] recent theoretical[19] and experimental[20] studies suggested that in the case of a (2×4) GaAs (001) surface, the anisotropy is mainly related to bulk states perturbed by the surface, rather than to the surface dimers. The controversy arises in part from the fact that the main features of the GaAs surface optical anisotropy, located around 2.89 eV, lie only 30 meV below the E_1 GaAs bulk transition, thus making it difficult to separate bulk and surface contributions.

In this paper, we address this problem by investigating the optical response of GaAs surface QW's (SQW's) consisting of a thin GaAs layer embedded between an arsenic-reconstructed surface and an AlAs barrier, as illustrated in Fig. 1. The motivation for the study lies on the fact that extended bulklike electronic states, which correspond in the present case to conventional QW confined states, can be considerably modified by varying the SQW thickness.[21,22] In contrast, highly localized surface states, such as those expected for dimer transitions, should be rather insensitive to confinement as long as their penetration depth remains shorter than the SQW thickness. The SQW thickness thus provides a length scale to probe the spatial extension of the surface states. By investigating the RDS response of SQW's with different thicknesses, one should be able to separate the bulklike contributions from the surfacelike contributions.

The RDS spectra of the SQW structures, however, are considerably more complex than that of the single GaAs surface, because each interface is intrinsically anisotropic and thus contributes to the total anisotropy.[23,24] This point becomes clear by examining the interfacial bonding arrangements illustrated in Fig. 1. While within each layer the anions are surrounded by four equivalent cations, the interfacial anion (As, black circles) is bonded to different cations from the upper and lower layers. The planes of the As-Al and As-Ga bonds involving a common anion are rotated by $\pi/2$ with respect to each other at each side of the interface. Consequently, different polarizabilities are expected along the $[\bar{1}10]$ and $[110]$ directions.[25]

The difficulties introduced by the interface anisotropy can be overcome by comparing RDS spectra for SQW's with

 ©2001 The American Physical Society

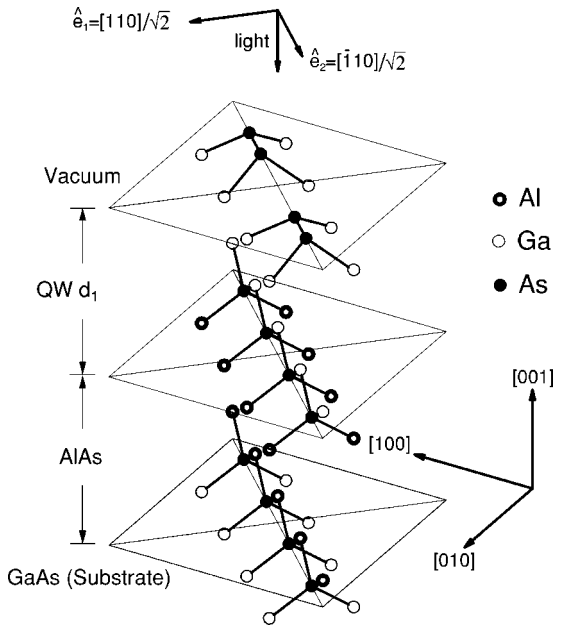

FIG. 1. Structure of the surface quantum-well samples. The GaAs SQW of thickness d_1 is embedded between an AlAs barrier and an As reconstructed surface. The As anion at each interface (black circle) is bonded to different cations from the layers below and above the interface. As a result, different polarizabilities are expected along the [110] and $[\bar{1}10]$ directions. The surface shows As dimers corresponding to a (2×4) reconstruction.

different surface reconstructions. Here we will concentrate on the $c(4\times4)$ and (2×4) GaAs (001) reconstructions. While the anisotropy related to the surface changes with reconstruction, the component associated with the buried interfaces is expected to be reconstruction independent, as long as the penetration depth of the surface states remains smaller than the SQW thickness. This procedure is justified by a multilayer formalism for the optical response (to be presented in Sec. II A), which takes into account multiple reflections at the buried interfaces. A further advantage of the procedure is that first-order contributions to the RDS signal from defects like dislocations,[12] and from surface electric fields,[26] are also eliminated.

RDS studies reveal that the optical anisotropy close to the E_1 transition also contains a contribution from bulk states rather than being of purely surface character. The bulk contribution is attributed to the mixing of the E_1 bulk states by the anisotropic strain field produced by the surface dimers.[27,28] The strain field penetrates tens of monolayers in the bulk, thus perturbing the atomic positions in a region below the surface.[29,28] We develop a model for this source of anisotropy in the SQW's, which also takes into account the energy shifts and changes in oscillator strength of the E_1 and $E_1+\Delta_1$ transitions induced by quantum confinement.

This paper is organized as follows. In Sec. II we develop a model to describe the RDS response of the SQW samples, including the anisotropy of the interfaces and effects of surface strain and QW confinement. Section III describes the sample preparation and the experimental details. Section IV describes experimental RDS results for QW's with different thicknesses. In Sec. V we give a detailed discussion of the experiments using the model exposed in Sec. II. The main conclusions are summarized in Sec. VI.

II. THEORY

In this section, we first develop a formalism to describe the RDS response of multilayer structures with anisotropic surface and interfaces. In Sec. II B, a model is presented for the optical response of the SQW's near the E_1 transition, which takes into account the effects of confinement and of anisotropic strains. Both models will be used in Sec. V to interpret the experimental RDS data.

A. RDS signal from heterostructures

In order to describe the RDS response of the SQW structures of Fig. 1, we will assume that the anisotropy induced by the surface has a maximum value at the surface plane, and vanishes for depths exceeding a characteristic length L. A similar assumption will be made for the anisotropy introduced by each interface, which will be taken to be constrained within a $2L_i$-thick layer centered at the interface plane.[30] Outside this layer, the dielectric function is equal to that of the bulk constituents (GaAs or AlAs), so that the anisotropy becomes negligible.

The complex reflection coefficient of the structure in Fig. 1 composed of two films (described by the indices 1 and 2) on a substrate (index 3) is given by[31]

$$r=\frac{r_{01}+r_{12}e^{-2i\bar{\delta}_1}+r_{23}e^{-2i(\bar{\delta}_1+\bar{\delta}_2)}+r_{01}r_{12}r_{23}e^{-2i\bar{\delta}_2}}{1+r_{01}r_{12}e^{-2i\bar{\delta}_1}+r_{01}r_{23}e^{-2i(\bar{\delta}_1+\bar{\delta}_2)}+r_{12}r_{23}e^{-2i\bar{\delta}_2}}, \tag{1}$$

where $\bar{\delta}_l$ is the average phase factor given by $2\pi\bar{n}_l d_l/\lambda$, λ is the light wavelength, $\bar{n}_l=(1/d_l)\int_0^{d_l} n_l(z)dz$ is the complex refractive index averaged over the thickness d_l of layer l, and $z||[001]$ is the coordinate along the growth direction. The complex reflection coefficient at the interface between the l and m media is defined by $r_{lm}=(n_m-n_l)/(n_m+n_l)$.

We have defined Eq. (1) in terms of average phase factors δ_l's since, in general, the refractive index for the lth material is not inhomogeneous along z. Around an interface, the refractive index is expected to become anisotropic as a consequence of the reduction of symmetry. The average change in refractive index for the two polarization states (in our case between the $[\bar{1}10]$ and the [110] directions, see Fig. 1) can be written as

$$\overline{\Delta n_l}=\frac{L}{d_l}\left(\frac{1}{L}\int_0^L \Delta n_l(z)dz\right), \tag{2}$$

where we have used the fact that $\Delta n_l(z)=n_l^{[1\bar{1}0]}(z)-n_l^{[110]}(z)\approx0$ for $z>L$.

The RDS signal of the heterostructure is defined as the relative difference $\Delta r/r$ between the complex reflection coefficient for polarizations along the [110] ($r_{[110]}$) and $[\bar{1}10]$

($r_{[1\bar{1}0]}$) directions. $\Delta r/r$ can be expressed in terms of Δn_l and of the anisotropic reflection at each interface $\Delta r_{ll+1}/r_{ll+1}$, according to

$$\frac{\Delta r}{r}=\sum_{l=0}^{2}\frac{r_{ll+1}}{r}\frac{\partial r}{\partial r_{ll+1}}\frac{\Delta r_{ll+1}}{r_{ll+1}}+\sum_{l=1}^{2}\frac{1}{r}\frac{\partial r}{\partial \overline{n_l}}\overline{\Delta n_l}. \tag{3}$$

Equation (3) includes contributions from the surface and from buried interfaces. In order to extract information about the surface contribution, a knowledge of the optical anisotropy induced by each individual interface is required. If the thickness L of the anisotropic surface layer is much smaller than the SQW thickness, the surface contribution can be distinguished from that of the interfaces by comparing RDS spectra for two different reconstructions, since the interface contribution does not depend on reconstruction. From Eq. (3) we obtain the following expression for the difference between the RDS spectra for the $c(4\times4)$ and the (2×4) reconstructions:

$$\left.\frac{\Delta r}{r}\right|_{c(4\times4)}-\left.\frac{\Delta r}{r}\right|_{(2\times4)}=\frac{r_{01}}{r}\frac{\partial r}{\partial r_{01}}\left[\left.\frac{\Delta r_{01}}{r_{01}}\right|_{c(4\times4)}-\left.\frac{\Delta r_{01}}{r_{01}}\right|_{(2\times4)}\right]+\frac{1}{r}\frac{\partial r}{\partial \overline{n_1}}[\overline{\Delta n_1}|_{c(4\times4)}-\overline{\Delta n_1}|_{(2\times4)}]. \tag{4}$$

Note that this expression depends only on the changes in the reflection coefficient Δr_{01} and in the refractive index anisotropy ($\overline{\Delta n_1}$) of the first layer induced by the reconstruction.

Δn_1 can be directly related to the RDS signal $\Delta r_{01}/r_{01}$ of the single GaAs surface following the formalism developed in Ref. 32. For this purpose, we assume that reconstruction leads to different projections of the dielectric tensor $\epsilon_{(1)}^{(j)}(z)$ along $j=[110]$ and $[1\bar{1}0]$. $\Delta r_{01}/r_{01}$ can then be expressed in terms of the dielectric anisotropy $\Delta\epsilon_{(1)}(z)=\epsilon_{(1)}^{[1\bar{1}0]}(z)-\epsilon_{(1)}^{[110]}(z)$ according to[32]

$$\frac{\Delta r_{01}}{r_{01}}=\frac{-2ik_1L}{n_1(\epsilon_{(1)}-1)}\overline{\Delta\epsilon_{(1)}}, \tag{5}$$

where $k_1=2\pi n_1/\lambda$ and $\overline{\Delta\epsilon_{(1)}}=(1/L)\int_0^L\Delta\epsilon_{(1)}(z)dz$. This expression is valid in the limit $k_1L\ll1$. An immediate consequence of the z dependence of the dielectric function is the mixing of the real and imaginary part of $\Delta r_{01}/r_{01}$ and $\overline{\Delta\epsilon_{(1)}}$ through the i factor in Eq. (5).[33]

Using Eqs. (2), (4), and (5), and the relation $\Delta\epsilon_{(1)}(z)=2n_1\Delta n_1(z)$, we arrive at the following expression:

$$\left.\frac{\Delta r}{r}\right|_{c(4\times4)}-\left.\frac{\Delta r}{r}\right|_{(2\times4)}=\left(\frac{r_{01}}{r}\frac{\partial r}{\partial r_{01}}+\frac{i}{4r}\frac{(\epsilon_{(1)}-1)}{k_1d_1}\frac{\partial r}{\partial \overline{n_1}}\right)\times\left[\left.\frac{\Delta r_{01}}{r_{01}}\right|_{c(4\times4)}-\left.\frac{\Delta r_{01}}{r_{01}}\right|_{(2\times4)}\right]. \tag{6}$$

Equation (6) relates the changes in the RDS signal of the multilayer structures induced by the reconstruction (left-hand side) to the surface reflection anisotropy (the term in the square brackets). If confinement effects can be neglected, the latter corresponds to the RDS signal of the free GaAs surface for the two reconstructions. Equations (6) and (5) can be combined to yield the dielectric changes induced by the reconstruction:

$$L\overline{\Delta\epsilon_{(1)}}|_{c(4\times4)}-L\overline{\Delta\epsilon_{(1)}}|_{(2\times4)}=\left(\frac{1}{2n_1d_1}\frac{1}{r}\frac{\partial r}{\partial \overline{n_1}}-\frac{2k_1i}{n_1(\epsilon_1-1)}\frac{r_{01}}{r}\frac{\partial r}{\partial r_{01}}\right)^{-1}\times\left[\left.\frac{\Delta r}{r}\right|_{c(4\times4)}-\left.\frac{\Delta r}{r}\right|_{(2\times4)}\right]. \tag{7}$$

Equations (6) and (7) will be used in Sec. V to analyze the multiple reflection effects in the measured RDS spectra.

B. Optical anisotropy of QW's near the E_1 and $E_1+\Delta_1$ transitions

In bulk semiconductors, the E_1 and $E_1+\Delta_1$ transitions take place at the four equivalent Λ-point $\langle111\rangle$ wave vector directions, which will be denoted here by $a=[111]$, $b=[1\bar{1}\bar{1}]$, $c=[\bar{1}11]$, and $d=[11\bar{1}]$. The electronic wave function of the conduction band will be denoted by $|S_i\rangle$, and those of the spin-orbit split valence states by $|L_i^{\pm}\rangle$, ($i=a$, b, c, and d), where the superscripts $+$ and $-$ will be used throughout to indicate states associated with the E_1 and $E_1+\Delta_1$ transitions, respectively. The states $|L_i^{\pm}\rangle$ can be expressed in terms of orbitals oriented along $\tilde{x}=[110]/\sqrt{2}$, $\tilde{y}=[\bar{1}10]/\sqrt{2}$, and $\tilde{z}=[001]$ for the four equivalent $\langle111\rangle$ directions. Due to the fourfold symmetry around the $\tilde{z}$ axis, in this section we only need to consider the $|L_a^{\pm}\rangle$ and $|L_c^{\pm}\rangle$ states, which can be written in terms of the orbitals $|\tilde{x}\rangle$, $|\tilde{y}\rangle$, and $|\tilde{z}\rangle$ as

$$|L_a^{\pm}\rangle=\frac{1}{\sqrt{2}}[-\sin\theta|\tilde{x}\rangle\pm i|\tilde{y}\rangle+\cos\theta|\tilde{z}\rangle],$$

$$|L_c^{\pm}\rangle=\frac{1}{\sqrt{2}}[|\tilde{x}\rangle\pm i\sin\theta|\tilde{y}\rangle\pm i\cos\theta|\tilde{z}\rangle], \tag{8}$$

where $\theta=\cos^{-1}(\sqrt{2/3})$.

The quantum confinement in QW's will affect the energy of the $|S_i\rangle$ and $\tilde{z}$ orbitals. The changes can be taken into account in a perturbation approach by defining a perturbation Hamiltonian ΔH_{cp}. Assuming infinite confinement barriers and a two-dimensional critical point for the E_1 transitions (a longitudinal mass much larger than the transverse mass), the matrix elements of ΔH_{cp} (in atomic units) become[34]

$$\cos^2\theta\langle\tilde{z}_i|\Delta H_{cp}|\tilde{z}_j\rangle=\delta_z=\delta_{ij}\frac{\cos^2\theta}{2m_v}\left(\frac{\pi}{d_1}\right)^2,\quad i,j=a,c \tag{9}$$

and

$$\langle S|\Delta H_{cp}|S\rangle = \delta_s = \frac{\cos^2\theta}{2m_c}\left(\frac{\pi}{d_1}\right)^2, \tag{10}$$

where d_1 is the QW thickness and m_v (m_c) is the transverse mass of the valence (conduction) band.

The contributions of the E_1 and $E_1+\Delta_1$ transitions to the dielectric function $\varepsilon_{(1)}$ of the SQW's is obtained by taking into account the mixing of the $|L_i^{\pm}\rangle$ states expressed by Eq. (9), and calculating the corresponding matrix elements to the L-point conduction band $|S_i^{\pm}\rangle$. We obtain the following expression for the average contribution $\overline{\varepsilon}_{(1)}^{\pm}(E)$ for $\tilde{x}$ and $\tilde{y}$ polarizations:

$$\overline{\varepsilon}_{(1)}(E) = \frac{1}{2}[\varepsilon_{(1)}^{\tilde{x}} + \varepsilon_{(1)}^{\tilde{y}}] = M^{\pm}\varepsilon_{(1)}(E, E_1 + \Delta E + i\Gamma), \tag{11}$$

where Γ is a phenomenological broadening parameter associated with the transition. The function ε describes the line shape of the E_1 contribution to the dielectric function; it differs from that in bulk materials since the confinement also changes the dimensionality of the transition. The confinement induces an energy shift $\Delta E^{\pm}$ and a transfer in oscillator strength $M^{\pm}$ between the E_1 and $E_1+\Delta_1$ components given by

$$\Delta E^{\pm} = \frac{\Delta_1}{2} \pm \frac{-\Delta_1}{2} + \frac{\delta_s+\delta_z}{2} \pm \frac{-\delta_z^2}{4\Delta_1} \tag{12}$$

and

$$M^{\pm} = \left[1 \pm \frac{-\delta_z}{2\Delta_1}\right], \tag{13}$$

where Δ_1 denotes the spin-orbit splitting.

While the confinement potential breaks the crystal symmetry, it preserves the fourfold symmetry around $\tilde{z}$, so that no anisotropy is induced in the $\tilde{x}$-$\tilde{y}$ plane. The array of As dimers[5] on the reconstructed (001) GaAs surface produce an anisotropic strain field that penetrates into the crystal.[27,29] This strain field lifts the fourfold symmetry and introduces an optical anisotropy into the $\tilde{x}$-$\tilde{y}$ plane. Its effect will be described by the anisotropic perturbation Hamiltonian ΔH_{ap} acting on the $|S_i\rangle$ and $|L_i^{\pm}\rangle$ bulk eigenstates. ΔH_{ap} mainly affects the orbitals $|\tilde{x}_i\rangle$ and $|\tilde{y}_i\rangle$ in the plane of the layers according to

$$\langle \tilde{x}_i|\Delta H_{ap}|\tilde{x}_j\rangle = \delta_{\tilde{x}}, \quad \langle \tilde{y}_i|\Delta H_{ap}|\tilde{y}_j\rangle = \delta_{\tilde{y}}, \quad i,j = a,c, \tag{14}$$

where $\delta_{\tilde{x}}$ and $\delta_{\tilde{y}}$ are phenomenological parameters which depend on the structure of the anisotropic surface layer.

When the spin-orbit interaction is included, the differences in oscillator strength $\Delta M^{\pm}$ (proportional to the squared matrix elements) for polarization along the $[\bar{1}10]$ and $[110]$ directions becomes[35]

$$\frac{\Delta M_a^{\pm}}{M} = \left[1 \pm 2\frac{\delta_{a12}}{\Delta_1}\right],$$

$$\frac{\Delta M_c^{\pm}}{M} = \left[-1 \pm 2\frac{\delta_{c12}}{\Delta_1}\right], \tag{15}$$

where

$$\delta_{a12} = +\delta_{\tilde{x}}\sin^2\theta - \delta_{\tilde{y}},$$

$$\delta_{c12} = +\delta_{\tilde{x}} - \delta_{\tilde{y}}\sin^2\theta. \tag{16}$$

By adding the contributions of transitions a to c and assuming $\delta_{\tilde{x}}$, $\delta_{\tilde{y}} \ll \Gamma$, the dielectric anisotropy becomes

$$\frac{\Delta\overline{\varepsilon}_{(1)}}{\overline{\varepsilon}_{(1)}} = \frac{\delta_{\tilde{y}}-\delta_{\tilde{x}}}{6}\left[\pm\frac{8}{\Delta_1} - \frac{1}{\overline{\varepsilon}_{(1)}E^2}\frac{\partial[E^2\overline{\varepsilon}_{(1)}]}{\partial E}\right]. \tag{17}$$

This equation describes the RDS line shape due to the anisotropic Hamiltonian defined by Eq. (14). It will be used together with Eq. (7) and Eqs. (11) in Sec. III to calculate the optical anisotropy.

III. EXPERIMENTAL DETAILS

The SQW's were grown by MBE on *n*-doped (10^{18} cm^{-3}) GaAs (001) substrates. The sample structure consists (cf. Fig. 1) of a homoepitaxial GaAs buffer layer (0.3 μm), an AlAs layer (10 nm) acting as the lower barrier, and a SQW with thickness d_1 ranging from 3 to 30 nm. The SQW's were capped with an As_2 protective layer (70 nm) deposited from a GaAs decomposition source. In order to obtain the optical response of the pure GaAs surface, a sample consisting of a single GaAs buffer layer capped As was also grown.

After growth, the samples were transferred in air to an ultrahigh-vacuum chamber with special windows for optical studies. The $c(4\times4)$- and (2×4)-reconstructed surfaces were obtained by annealing the samples at 320 and at 430 °C, respectively, to adsorb the As cap layer.[36] The As adsorption process was monitored *in situ* by measuring the pseudo-dielectric function during annealing by ellipsometry. In view of the large difference between the dielectric function of the capped and cleaned surfaces around the GaAs E_2 transitions (approximately 4.5 eV), this procedure ensured a reproducible preparation of the $c(4\times4)$ surface reconstruction.[36] Likewise, we have used RDS (around 2.89 eV) to monitor the change in reconstruction, from $c(4\times4)$ to 2×4. After annealing, the samples were cooled to room temperature for the subsequent RDS and ellipsometric measurements.

The experiments were performed using a rotating analyzer ellipsometer[37] and a RDS spectrometer[38] based on a photoelastic modulator (Hinds PEM80). The illumination system consists of a 75-W Xenon lamp (Hamamatsu L2174) and a double monochromator (Spex 1680) operated with a spectral resolution of 2.25 nm. UV-Rochon prisms were used as polarizers, and the signal was detected by a S-20-type photomultiplier. The RDS spectra were recorded in the en-

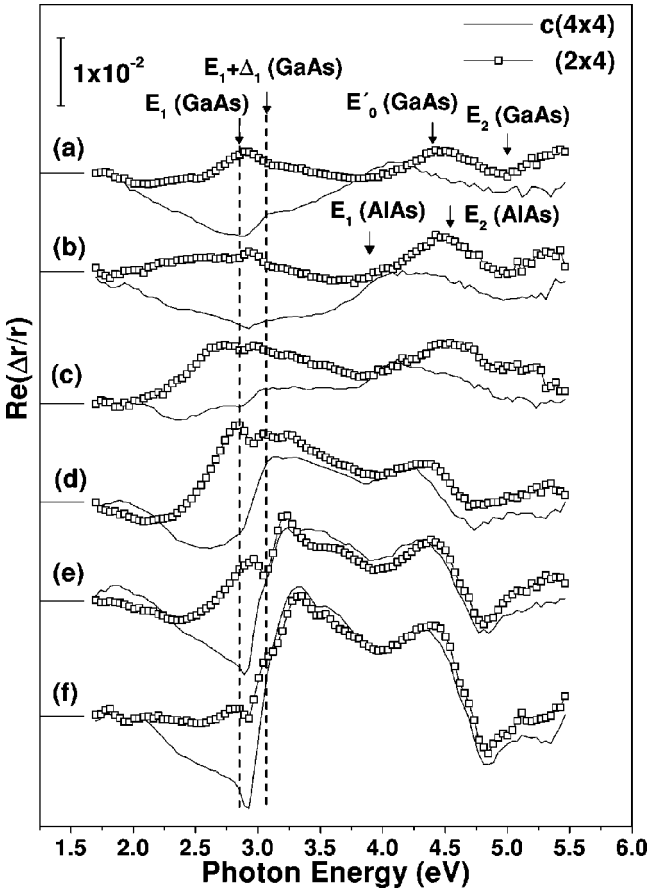

FIG. 2. Real part of the RDS spectra of (a) (001) GaAs, and of GaAs SQW's with thicknesses of (b) 30 nm, (c) 20 nm, (d) 10 nm, (e) 5.3 nm, and (f) 3 nm. In each case, spectra are shown for the $c(4\times4)$- (lines) and for the (2×4)-(filled squares) surface reconstructions, respectively. The RDS signal $\Delta r/r$ is defined as the relative difference between the complex reflection coefficient for polarizations along the $[\bar{1}10]$ ($r_{[\bar{1}10]}$) and $[110]$ ($r_{[110]}$) directions.

ergy range from 1.7 to 5.5 eV. The real and imaginary parts of the reflection anisotropy $\Delta r/r$ were measured simultaneously by detecting the reflected intensity at the first and second harmonics of the modulator frequency.

IV. EXPERIMENTAL RESULTS

Figure 2 shows the real part of the RDS spectra for the $c(4\times4)$- (lines) and (2×4)- (squares) reconstructed surface for pure GaAs (a) and for SQW's with different thicknesses (b)–(f). The spectrum for the GaAs surface [Fig. 2(a)] is similar to those previously reported.[5] Most prominent is the broad anisotropic feature centered around 2.89 eV, which has opposite signs for the two reconstructions. This feature has been assigned to transitions involving surface As dimers,[5] which have different orientations for the two reconstructions.

For large SQW thicknesses (i.e., thicknesses above 30 nm), the RDS spectra are essentially equal to those of the GaAs surface, since the incoming light is strongly absorbed in the SQW layer and confinement effects are negligible. For thinner SQW's, considerable modifications are observed. The

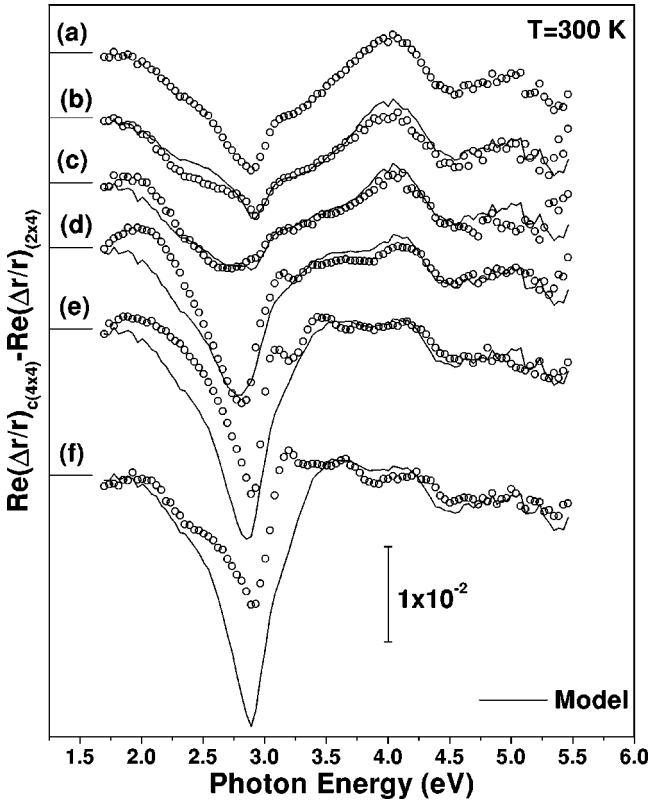

FIG. 3. Difference between RDS spectra for the $c(4\times4)$ and (2×4) reconstructions (cf. Fig. 2) for (a) the free GaAs surface and for SQW's with thicknesses of (b) 30 nm, (c) 20 nm, (d) 10 nm, (e) 5.3 nm, and (f) 3 nm. The solid lines were calculated using Eq. (6).

dimer-dimer transition (around 2.8 eV) with a convex (concave) line shape for $c(4\times4)$ $[(2\times4)]$ is still the dominant one in the low energy region: the precise line shape, however, depends strongly on the SQW thickness. Also, strong features develop close to the E_1 and $E_1+\Delta_1$ transitions.

For energies above the $E_1+\Delta_1$ transition, the RDS spectra of thin SQW's become essentially insensitive to surface reconstruction. In the thinner samples [Fig. 2(f)], the changes with reconstruction only appear for energies below 3.0 eV. The spectra are dominated by features at the energies of the bulk critical points of GaAs ($E_1+\Delta_1$, E_0', and E_2) and AlAs (E_0, E_1, and E_2), thus indicating a strong contribution from buried layers and interfaces.

V. DISCUSSION

As discussed in Sec. II, the RDS spectra of the SQW's in Fig. 2 include contributions from the surface as well as from the buried interfaces. In order to separate the two contributions and to access the surface contribution following the procedure described in Sec. II, we calculated the numerical difference between the RDS spectra for the $c(4\times4)$ and (2×4) reconstructions. The result is displayed by the circles in Fig. 3. The spectra show systematic changes with decreasing SQW width, which are more pronounced around the critical points E_1 of the GaAs (around 3 eV) and E_1 of AlAs (around 4 eV).

According to the discussion in Sec. II, in the absence of confinement effects the difference spectra in Fig. 3 can be directly related to the anisotropy of the GaAs $c(4\times4)$- and the (2×4)-reconstructed surfaces. The solid lines superimposed on the experimental data in Fig. 3 display the difference spectra calculated from Eq. (6) using the measured anisotropy of the $c(4\times4)$ and the (2×4) GaAs surfaces shown in Fig. 3(a). The first term on the right-hand side of Eq. (6) was calculated using the dielectric functions of GaAs measured by ellipsometry and the reported values of the dielectric function of AlAs.[39]

For wide SQW's [as in Figs. 3(b)–3(d)], confinement effects are expected to be negligible (energy shifts less than 10 meV). Accordingly, the solid lines reproduce well the measured spectra over the whole spectral range, thus demonstrating that Eq. (6) correctly takes into account multiple reflection effects at the buried interfaces. In addition, the calculations reproduce quite well the measured spectra for energies above 4.0 eV over the whole range of SQW thicknesses. We attribute this behavior to the fact that (i) the high-energy transitions in GaAs and AlAs are less sensitive to confinement effects;[21] and that (ii) according to the calculations obtained using Eq. (6), above 4.3 eV the buried barriers do not contribute significantly to the RDS signal of the SQW's.

A question arises as to whether we are within the limit $k_1L\ll1$ that is the limit of validity of Eq. (5). An analytical equation correct for any value of k_1L is unfortunately not available. Thus, to answer this question we have redone the fits for the equation appropriate to the opposite limit $k_1L\gg1$.[20] We found that they were considerably poorer. We believe that this is enough of an argument to use Eq. (5) as a plausible approximation.

The calculations, however, fail to reproduce the line shape and the intensity of difference spectra for the thinner SQW samples [Figs. 3(e)–3(f)] for energies below 3.5 eV. In this energy range, the calculations predict a strong enhancement in intensity of the structures associated with the surface anisotropy, which occurs due to constructive interference effects in the buried interfaces. Such an enhancement is not observed in the experimental data. In addition, the calculations do not reproduce the dip and the maximum at the energies of the E_1 and $E_1+\Delta_1$ transitions of GaAs, respectively, which become more pronounced in the measured spectra for decreasing SQW thickness. The anisotropy around the E_1 transitions will be discussed in detail below.

Finally, in addition to the E_1 and $E_1+\Delta_1$ features, the spectra comprise an additional component that adds a negative offset to the E_1 and $E_1+\Delta_1$ oscillations. This additional component tends to zero faster than the amplitude of the E_1 and $E_1+\Delta_1$ transitions, as can be seen for the 3-nm sample in Fig. 3(f), where the structure for the E_1 $(E_1+\Delta_1)$ peak takes negative (positive) values contrasting, for instance, with the spectrum of Fig. 3(a) that takes only negative values around these transitions. This additional component could be related to surfacelike states. These states penetrate into the bulk ≈8 nm.[40] As seen in Fig. 3, the strength of the additional component for spectra (a), (b), (c) and (d) remains unchanged, in agreement with this penetration depth. For the thinner QW's, the reduction of the strength may be related to the interaction between surface states and the buried interface.[40]

The calculated solid lines in Fig. 3 only take into account the anisotropy of the free GaAs surface and the effects of multiple light reflection at the buried interfaces. For thinner SQW's the discrepancy between calculated and measured line shapes increases. The discrepancy is partially related to the energy shifts due to confinement effects, which become important for the thinner SQW samples. Another factor that was not taken into account in previous calculations is the relative values for the thickness of the anisotropic layer (L), of the SQW (d_1), and the light penetration depth. If L or the penetration depth (whichever is smaller) exceeds d_1, then a reduction of the strength of the RDS features is expected. In any cases, these results clearly demonstrated that the anisotropy observed in Figs. 2 and 3 cannot be attributed to highly localized surface states with localization lengths of a few Å's.

In order to address the mechanisms responsible for the anisotropy in the SQW's, it is convenient to represent the anisotropy in terms of the changes in the dielectric function using Eq. (7). The imaginary part of $L\overline{\Delta\epsilon_1}|_{c(4\times4)}-L\overline{\Delta\epsilon_1}|_{(2\times4)}$, obtained from the experimental results of Fig. 3, is shown in Fig. 4. Note that spectra (a), (b), and (c) are practically the same, thus indicating again that the multiple reflections model of Eq. (7) correctly takes into account the contribution of the buried layers. For thinner SQW's the effects discussed above are important, and the change in line shape becomes evident.

We now address the contributions of the E_1 and $E_1+\Delta_1$ GaAs transitions to the optical anisotropy of the SQW's following the procedure delineated in Sec. II B. For that purpose, we fit the measured data around the E_1 and $E_1+\Delta_1$ transitions to Eq. (17) (lines in Fig. 4). The line-shape function $\overline{\varepsilon}_{(1)}$ necessary for the fit [cf. Eq. (11)] was obtained from the measured dielectric function of the clean GaAs surface. From the fitting procedure, we obtain the parameters δ_z, δ_s, and $\delta_y^{\sim}-\delta_x^{\sim}$, which describe the energy shifts, the oscillation intensities, and the anisotropy of the transitions [according to Eqs. (12), (13), and (14), respectively].

For pure GaAs [Fig. 4(a)] the fit reproduces quite well the line shape around E_1 and $E_1+\Delta_1$ transitions. In this case, only the amplitude of the transitions was taken as an adjustable parameter. The spectrum for the 10-nm SQW in Fig. 4(d) was fitted using the same amplitude as before, but including a blue energy shift of 10 ± 3 meV for the E_1 and $E_1+\Delta_1$ transitions. For the spectra in Figs. 4(e) and 4(f), blue energy shifts of 19 ± 3 and of 38 ± 3 meV were obtained, respectively. The fitted energy shifts are displayed as a function of the SQW thickness in Fig. 5 (circles). The squares in the same plot show the confinement-induced energy in (001)-oriented GaAs/AlAs multiple QW's measured by Garriga *et al.*[21] using spectroscopic ellipsometry. Note the scatter in the data of Ref. 21 for QW widths exceeding 2 nm, much larger than the error bars of our measurements. We attribute this difference to the fact that RDS is a more sensitive technique than ellipsometry.

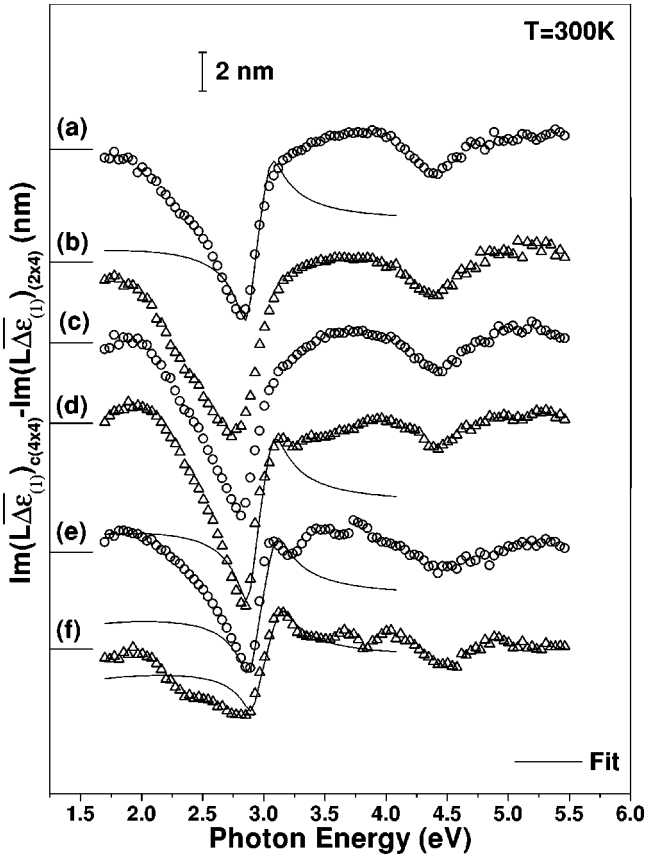

FIG. 4. Imaginary part of the dielectric anisotropy $L\overline{\Delta\epsilon_1}|_{c(4\times4)}-L\overline{\Delta\epsilon_1}|_{(2\times4)}$ obtained using Eq. (7) for (a) a GaAs surface and for SQW's with thicknesses of (b) 30 nm, (c) 20 nm, (d) 10 nm, (e) 5.3 nm, and (f) 3 nm. The solid lines show the contribution from the E_1 and $E_1+\Delta_1$ transitions calculated using Eq. (7).

The dependence of the energy shift with the QW thickness is given by Eqs. (9) and (10). These equations were obtained assuming infinite barriers, and thus are expected to give values that largely exceed the experimental ones. However, the shift follows the $1/d_1^2$ dependence (solid line) as can be seen in Fig. 5.

The fits of Figs. 4(a) and 4(d) yield the same oscillator intensity for the E_1 and $E_1+\Delta 1$ transitions. In Figs. 4(e) and 4(f), the amplitude of the spectra begins to decrease with respect to spectra (a) and (d). This suggests that the thickness of the anisotropic layer should be smaller than 10 nm. Assuming that for these two spectra $d_1=L$, the amplitude of the RDS should become proportional to the QW thicknesses. The ratio between the maximum to minimum amplitudes of the solid lines of spectra (e) and (f) is equal to 0.71 ± 0.07. This ratio agrees reasonably well with the estimated SQW thickness ratio of 0.565 ± 0.065, where the error bars were obtained taking into account an error of ± 2 Å in the QW's thicknesses.

The energy difference $\delta_{\tilde{y}}-\delta_{\tilde{x}}$ reflects the reduction in symmetry of the E_1 states induced by the reconstructed surface. Using Eq. (17) and the fitted amplitude for the spectrum of Fig. 4(a) we have estimated $L(\delta_{\tilde{y}}-\delta_{\tilde{x}})\approx 0.07$ eV nm. Taking $L=5$ nm, in accordance with the discussion of the previous paragraph, we obtain $\delta_{\tilde{y}}-\delta_{\tilde{x}}\approx 14$ meV. We attribute the energy difference $\delta_{\tilde{y}}-\delta_{\tilde{x}}$ to an effective shear strain e_{xy} induced in the SQW's by the surface dimers.[28] The amplitude of the anisotropic strain can be related to $\delta_{\tilde{y}}-\delta_{\tilde{x}}$ by[35]

$$e_{xy}=\frac{\delta_{\tilde{y}}-\delta_{\tilde{x}}}{3^{1/2}2d}, \tag{18}$$

where e_{xy} is the magnitude of the anisotropic strain referred to by the crystal axes, and d is the uniaxial deformation of rhombohedral symmetry. Taking $d=-5.4$ eV for GaAs,[41] from Eq. (18) we estimate a surface strain of $e_{xy}\approx 7.5\times10^{-4}$.

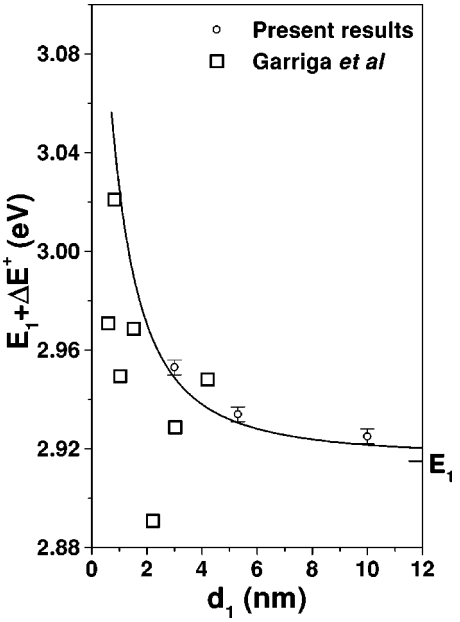

FIG. 5. Energy shift of the E_1 transition of GaAs vs QW thickness. The plot shows literature data (squares) and the results of the present work (circles). For QW's of 20 and 30 nm, we obtained a shift of 1 ± 3 meV. The curve is a fit to $1/d_1^2$.

VI. CONCLUSIONS

We have measured the RDS spectra of (001)-oriented QW's (3, 5.3, 10, 20, and 30 nm thick) with the asymmetric structure As dimers/GaAs-QW/AlAs/GaAs(buffer) for $c(4\times4)$ and (2×4) surface reconstructions. The model to describe the surface anisotropy developed in the present work is based on the anisotropic strain field produced by the dimers. This strain perturbs the electronic energy levels and the intensities of the E_1 and $E_1+\Delta_1$ transitions. In the model we have taken into account confinement and multiple reflections. We show that the RDS spectra around 3.0 eV consist mainly of two contributions: a broad structure and a sharp structure, attributed to surfacelike and bulklike transitions, respectively.

ACKNOWLEDGMENTS

We would like to thank H. Hirt, P. Hiessl, M. Siemers, and W. Stiepany for technical assistance and J. Kuhl for a critical reading of the manuscript. This work was supported by Fonds der Chemischen Industrie.

*Email address: lflm@cactus.iico.uaslp.mx

[1] D. E. Aspnes and A. A. Studna, Phys. Rev. Lett. **54**, 1956 (1985).
[2] W. L. Mochan and R. G. Barrera, Phys. Rev. Lett. **55**, 1192 (1985).
[3] R. Del Sole, W. L. Mochan, and R. G. Barrera, Phys. Rev. B **43**, 2136 (1991).
[4] Y. C. Chang, S. F. Ren, and D. E. Aspnes, J. Vac. Sci. Technol. A **10**, 1856 (1992).
[5] I. Kamiya, D. E. Aspnes, L. T. Florez, and J. P. Harbison, Phys. Rev. B **46**, 15 894 (1992).
[6] M. Murayama, K. Shiraishi, and T. Nakayama, Jpn. J. Appl. Phys. **37**, 4109 (1998).
[7] A. I. Shkrebtii, N. Esser, W. Richter, W. G. Schmidt, F. Bechstedt, B. O. Fimland, A. Kley, and R. Del Sole, Phys. Rev. Lett. **81**, 721 (1998).
[8] D. E. Aspnes, J. Vac. Sci. Technol. B **3**, 1498 (1985).
[9] D. E. Aspnes and A. A. Studna, J. Vac. Sci. Technol. A **5**, 546 (1987).
[10] S. E. Acosta-Ortíz and A. Lastras-Martínez, Phys. Rev. B **40**, 1426 (1989).
[11] S. E. Acosta-Ortíz and A. Lastras-Martínez, Proc. SPIE **1286**, 31 (1990).
[12] L. F. Lastras-Martínez and A. Lastras-Martínez, Phys. Rev. B **54**, 10 726 (1996).
[13] B. Koopmans, P. V. Santos, and M. Cardona, Phys. Status Solidi A **170**, 307 (1998).
[14] L. F. Lastras-Martínez, P. V. Santos, D. Rönnow, M. Cardona, P. Specht, and K. Eberl, Phys. Status Solidi A **170**, 317 (1998).
[15] D. E. Aspnes, J. P. Harbison, A. A. Studna, L. T. Florez, and K. Kally, J. Vac. Sci. Technol. B **6**, 1127 (1998).
[16] D. E. Aspnes, E. Colas, A. A. Studna, R. Bhat, M. A. Koza, and V. G. Keramidas, Phys. Rev. Lett. **61**, 2782 (1988).
[17] H. Tanaka, E. Colas, I. Kamiya, D. E. Aspnes, and R. Bhat, Appl. Phys. Lett. **59**, 3443 (1991).
[18] W. Gero Schmidt, F. Bechstedt, and G.P. Srivastava, Surf. Sci. Rep. **25**, 141 (1996).
[19] R. Eryigit and I. P. Herman, Phys. Rev. B **56**, 9263 (1997).
[20] U. Rossow, L. Mantese, and D. E. Aspnes, Appl. Surf. Sci. **123/124**, 237 (1998).
[21] M. Garriga, M. Cardona, N. E. Christensen, P. Lautenschlager, T. Isu, and K. Ploog, Phys. Rev. B **36**, 3254 (1987).
[22] U. Schmid, N. E. Christensen, M. Cardona, F. Lukeŝ, and K. Ploog, Phys. Rev. B **45**, 3546 (1992).
[23] O. Krebs and P. Voisin, Phys. Rev. Lett. **77**, 1829 (1996).
[24] O. Krebs, W. Seidel, J. P. André, D. Bertho, C. Jouanin, and P. Voisin, Semicond. Sci. Technol. **12**, 938 (1997).
[25] E. L. Ivchenko, A. Yu. Kaminski, and U. Rössler, Phys. Rev. B **54**, 5852 (1996).
[26] A. Lastras-Martínez, R. E. Balderas-Navarro, L. F. Lastras-Martínez, and M. A. Vidal, Phys. Rev. B **59**, 10 234 (1999).
[27] J. P. Silveira and F. Briones, J. Cryst. Growth **201/202**, 113 (1999).
[28] K. Hingerl, R. E. Balderas-Navarro, W. Hilber, A. Bonanni, and D. Stifter, Phys. Rev. B **62**, 13048 (2000).
[29] J. A. Appelbaum and D. R. Hamann, Surf. Sci. **74**, 21 (1978).
[30] T. Yasuda, Thin Solid Films **314-314**, 544 (1998).
[31] O. S. Heavens, *Optical Properties of Thin Solid Films* (Dover, New York, 1965) p. 63.
[32] D. E. Aspnes and A. Frova, Solid State Commun. **7**, 155 (1969).
[33] M. Kelly, S. Zollner, and M. Cardona, Surf. Sci. **285**, 282 (1993).
[34] See, e.g., P. Yu and M. Cardona, *Fundamentals of Semiconductors* (Springer, Berlin, 1996), p. 459.
[35] F. H. Pollak and M. Cardona, Phys. Rev. **172**, 816 (1968).
[36] N. Esser, P. V. Santos, M. Kuball, M. Cardona, M. Arens, D. Pahlke, W. Richer, F. Stietz, J. A. Schaefer, and B. O. Fimland. J. Vac. Sci. Technol. B **13**, 1 (1995).
[37] D. E. Aspnes, Opt. Commun. **8**, 222 (1973); D. E. Aspnes and A. A. Studna, Appl. Opt. **14**, 220 (1975); Rev. Sci. Instrum. **49**, 291 (1978).
[38] D. E. Aspnes, J. P. Harbison, A. A. Studna, and L. T. Florez, J. Vac. Sci. Technol. A **6**, 1327 (1988).
[39] *Handbook of Optical Constants of Solids II*, edited by E. D. Palik (Academic Press, New York, 1985).
[40] J. M. Moison, K. Elcess, F. Houzay, J. Y. Marzin, J. M. Gérard, F. Barthe, and M. Bensoussan, Phys. Rev. B **41**, 12 945 (1990).
[41] *Semiconductors Physics of Group IV Elements and III-V Compounds*, edited by O. Madelung, M. Schultz, and H. Weiss, Landolt-Börnstein, New Series, Group III, Vol. 17, Pt. a (Springer-Verlag, Berlin, 1982).